Supporting Information

Determination of defect levels in melt-grown all-inorganic perovskite $CsPbBr_3$ crystals by thermally stimulated current spectra

*Mingzhi Zhang [a], Zhiping Zheng [*a], Qiuyun Fu [a], Pengju Guo [a], Sen Zhang [a], Cheng Chen [a], Hualin Chen [a], Mei Wang [a], Wei Luo [a], Yahui Tian [a]*

[a] School of Optical and Electronic Information, Engineering Research Center for Functional Ceramics of the Ministry of Education, Huazhong University of Science and Technology, Wuhan 430074, P. R. China

Full affiliation address: No. 1037, Luoyu Road, Hongshan District, Wuhan, Hubei Province, P. R. China, 430074

Corresponding Author

* Zhiping Zheng

Email: zzp@mail.hust.edu.cn

Tel: +86-27-87545167

Fax: +86-27-87545167

Contents

Section 1. Crystal growth, crystal cutting, and wafer treatment

The growth of $CsPbBr_3$ single crystal ingots was conducted in a self-designed vertical two-zone tube furnace by a creative electronic dynamic gradient (EDG) method. [1] The melt-grown crystals had a size of over 60 mm in length with a middle isometric (ϕ8 mm) part of 40 mm. Wafers of around 2.5 mm thick were sliced along the radial direction from the isometric part using a 0.2 mm diamond wire saw.

Then the wafers were treated by a series of surface treatments to remove the physical damage and flatten the wafer surface. Si_3N_4 abrasives with 14 μm in diameter and then 7, 1.5 and 0.5 μm were used to polish the surfaces of the wafers in turns. After that, the polished wafers were immersed in a concentration of 5% bromine methanol solution for 30 s to remove the physical damage of the surface caused by the cutting and mechanical polishing processes. Wafers with bright, shiny and mirror-like surfaces were obtained.

Section 2. Theoretical formula analysis of TSC measurement and SIMPA method

The transition levels for different charged defect states were calculated using HSE+SPC by Jun Kang and Lin-Wang Wang, and the results were shown in Figure S1. [2]

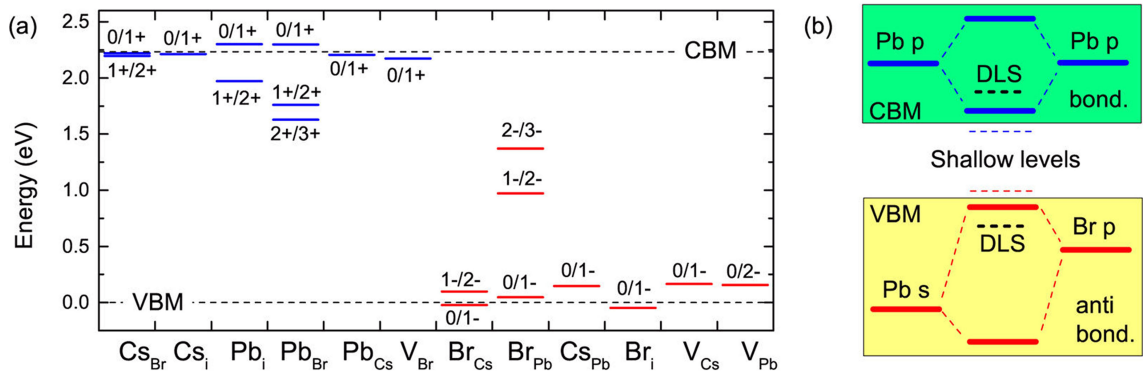

Figure S1. (a) Defect charge-transition levels calculated by HSE+SOC; (b) Illustration of the formation of shallow levels. Reprinted with permission from High Defect Tolerance in Lead Halide Perovskite $CsPbBr_3$. Copyright 2017, *American Chemical Society*.

In semiconductor materials, the kinetic equation of the concentration of electron (n_i) in deep level vs. time (t) can be expressed as Equation (1): [3]

$$\frac{dn_i}{dt} = -n_i N_C \sigma_i v_n \exp\left(-\frac{\Delta E_i}{k_0 T}\right) + n\left(N_i - n_i\right)\sigma_i v_n \tag{1}$$

Where, N_i is the concentration of the *ith* electronic defect, n_i is the concentration of electron occupied by the *ith* electronic defect, n is the concentration of electron in conduction band, ΔE_i is the defect level, σ_i is the capture cross section of the *ith* defect, v_n is the thermal velocity, N_C is the effective state density of electron, k_0 is the Boltzmann constant, T is the absolute temperature, and τ is the average carrier lifetime. In fact, most of thermal motivated carriers are captured by all kinds of recombination centers and only a small number of carriers can be re-captured by trapping centers, this means $\sigma_i \cdot v_n \ll 1/\tau$, then we get the Equation (2):

$$\frac{\Delta E_i}{k_0 T_m} = \ln\left(\frac{T_m^2}{\beta}\right) + \ln\left(\frac{N_C \sigma_i v_n k_0}{\Delta E_i}\right) \tag{2}$$

Where, T_m is peak temperature of TSC current, β is the heating rate of the TSC measurement. As the effective state density of electron (N_C) being inversely proportional to the square of temperature ($N_C \propto T^{-2}$), the Equation (2) can be also expressed as Equation (3):

$$\ln\left(\frac{T_m^4}{\beta}\right) = \frac{\Delta E_i}{k_0 T_m} - \ln\left(\frac{N_C \sigma_i v_n k_0}{\Delta E_i T^2}\right) \tag{3}$$

The capture cross section (σ_i) is usually very small in high resistance semiconductor single crystals, then the effect of the last expression in Equation (3) can be ignored, that is:

$$\Delta E_i = k_0 T_m \ln\left(\frac{T_m^4}{\beta}\right) \tag{4}$$

In the SIMPA fitting method, the temperature (T) dependence of TSC current, $I_{SIMPA}(T)$, comprising the sum of TSC peaks belonging to the specific levels and the dark current $I_{DC}(T)$, is defined by:

$$I_{SIMPA}(T) = \sum_{i=1}^{m} I_{TSC}^{i}(T) + I_{DC}(T) \tag{5}$$

Where, $I^i_{TSC}(T)$ is the *ith* individual TSC current peak, m is the number of defects involved in calculation. In the "first-order kinetics" approximation, the temperature (T) dependent TSC current $I^i_{TSC}(T)$ of a certain peak can be described as a specialized one:

$$I_{TSC}^{i}(T) = N_{T_i} e \mu_n A E \tau_n D_{t,i} T^2 \exp\left\{-\frac{E_{T_i}}{k_0 T} - \frac{k_0 D_{t,i} T^4}{\beta E_{T_i}} \exp\left(-\frac{E_{T_i}}{k_0 T}\right)\left[1 - 4\left(\frac{k_0 T}{E_{T_i}}\right) + 20\left(\frac{k_0 T}{E_{T_i}}\right)^2\right]\right\} \tag{6}$$

Where, N_T is the defect density at the beginning of temperature rising, e is the electron charge, μ is the carrier mobility, τ is the carrier lifetime, A is the area of electrode, E is the applied electric field, D_t is the defect dependent coefficient, T is the absolute temperature, E_T is the thermal activation energy of the *ith* defect which is related to the TSC peak position, k_0 is the Boltzmann constant, and β is the heating rate of the TSC measurement. In addition, $K_G = e\ A\ E$ denotes a

geometrical factor. The defect-dependent coefficient D_t has a relationship with the capture cross section σ_i , which can be expressed as:

$$D_t = 3.0 \times 10^{21} \left(\frac{m^*}{m_0} \right) \sigma_i \tag{7}$$

Where, m_0 is the rest mass of carries and m^* is the effective mass of carries which is calculated to be 0.23 m_0 for both holes and electrons at room temperature.

The *ith* effective collecting charge (Q_{Ti}) can be acquired from the SIMPA method. Q_{Ti} is time integral of the *ith* TSC current, and the expression can be described as:

$$Q_{T_i} = \int I_{TSC}^i dt = \frac{1}{\beta} \int_{T_0}^{T} I_{TSC}^i dT \leftarrow (dT = \beta dt) \tag{8}$$

Then the concentration (N_{Ti}) of the ith defect can be calculated by the Equation (9):

$$N_{T_i} = \frac{Q_{T_i}}{V_{eff} \times e \times G} \tag{9}$$

Where, V_{eff} ($V_{eff} = AL$) is the effective irradiation volume of the wafer, and G is the collecting efficiency which can be defined as:

$$G = \frac{\mu \tau V}{L^2} \tag{10}$$

Where, L is the distance of two Au electrodes, and V is the bias voltage.

Furthermore, a correction factor (f=1/2) is attached to the *ith* TSC current because of the uniform distribution of defects in the wafer. Then the concentration (N_{Ti}) of the ith defect can be expressed as:

$$N_{T_i} = \frac{Q_{T_i}}{2\mu \tau e A E} \tag{11}$$

Section 3. Calculation of carrier mobility lifetime product ($\mu\tau$) of melt-grown $CsPbBr_3$ crystals

In order to calculate the approximate concentration of intrinsic point defects in our melt-grown $CsPbBr_3$ crystals, the carrier mobility lifetime product ($\mu\tau$) are required.

Photocurrent measurements were conducted using Agilent B1500A equipped with a 325 nm pulsed laser. The measurements were carried out on $CsPbBr_3$ devices with a structure of Au/$CsPbBr_3$/Au. A modified Hecht equation (Equation (12)) was used to fit the obtained result, deriving the information of $\mu\tau$ product and surface recombination velocity S.

$$I = \frac{I_0 \mu\tau V}{L^2} \frac{1-\exp\left(-\frac{L^2}{\mu\tau V}\right)}{1+\frac{L}{V}\frac{S}{\mu}} \tag{12}$$

Where, I_0 is the saturated photocurrent, μ is the carrier mobility, τ is the carrier lifetime, V is the applied bias, and L is the thickness of the device. The fitting curves and results were shown in Figure S2 and Table S1, respectively.

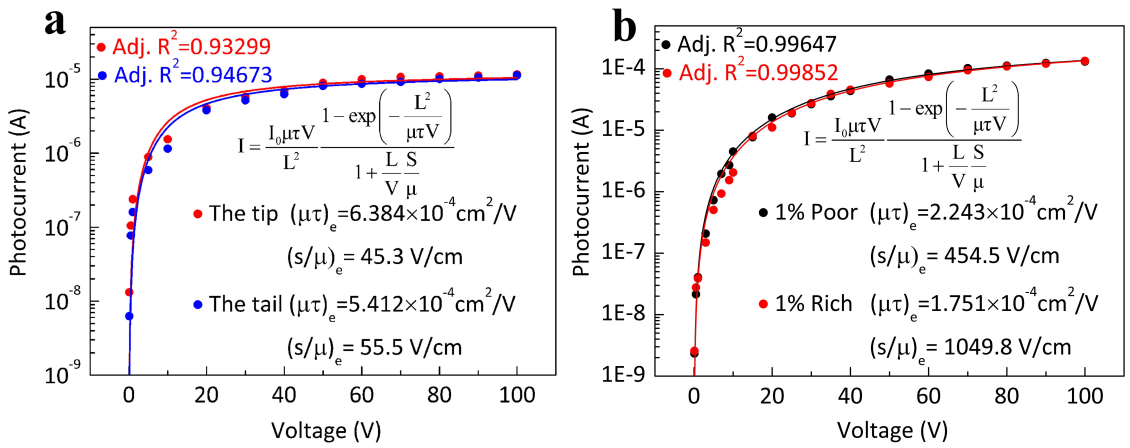

Figure S2. Bias-dependent photocurrent of two samples from (a) the tip and the tail part of a same ingot, (b) tip part of a 1% Pb-rich and a 1% Pb-poor crystal

Table S1 The fitting results in **Figure S2**

Sample	Tip region	Tail region	1% Pb-poor crystal	1% Pb-rich crystal
Thick (mm)	1.216	1.205	1.577	1.266
μτ (cm^2/V)	6.384×10^{-4}	5.412×10^{-4}	2.243×10^{-4}	1.751×10^{-4}
s/μ (V/cm)	45.3	55.5	454.5	1049.8

Section 4. Defect-related fitting parameters of TSC spectra

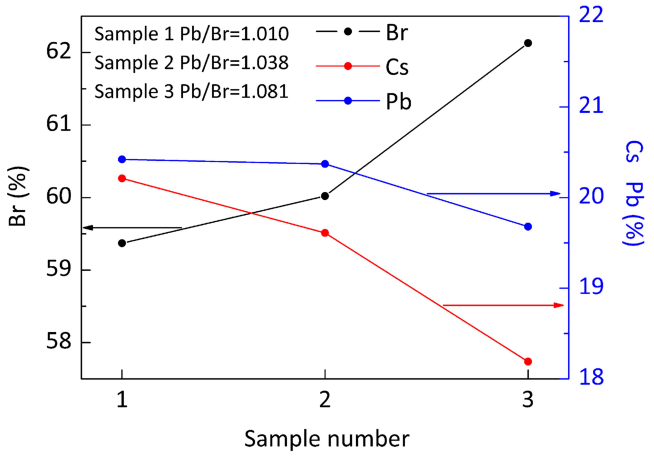

Figure S3. Elemental ratio of wafer as a function of regions of a same crystal

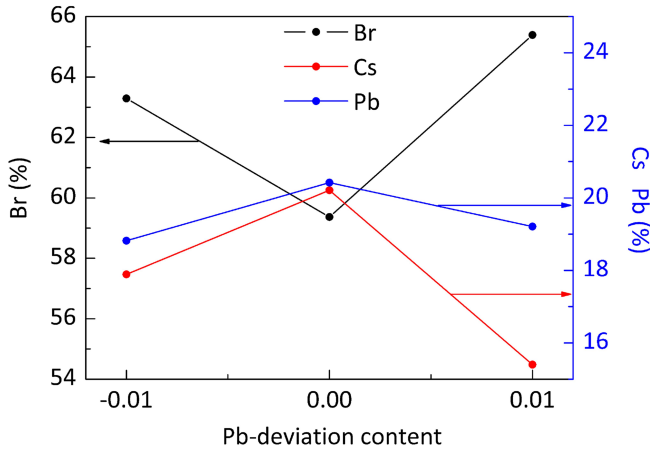

Figure S4. Elemental ratio in $CsPbBr_3$ crystals as a function of stoichiometric condition (1% Pb-poor, stoichiometric and 1% Pb-rich)

Table S2. Structure parameters of $[PbBr_6]$ octahedra in three structures

Parameter	Bond distance (Å)			Bond angle (°)			Volume
Crystal structure	$(Pb\text{-}Br)_{//a}$	$(Pb\text{-}Br)_{//b}$	$(Pb\text{-}Br)_{//c}$	$(Br\text{-}Pb\text{-}Br)_{//\alpha}$	$(Br\text{-}Pb\text{-}Br)_{//\beta}$	$(Br\text{-}Pb\text{-}Br)_{//\gamma}$	V (Å^3)
Orthorhombic	2.955(8)	2.984(8)	2.964(2)	90.8(2)	90.2(2)	89.67(14)	34.84 (3%↑)
Tetragonal	2.930(2)	2.930(2)	2.723(4)	91.3833(0)	91.3833(0)	89.9666(0)	31.15 (8%↓)
Cubic	2.9370(10)	2.9370(10)	2.9370(10)	90(0)	90(0)	90(0)	33.78 (Std.)

Table S3. Defect-related parameters based on the best fit of a typical TSC spectrum of a sample from the tip part of a stoichiometric $CsPbBr_3$ ingot

Peak level (T)		T_m / K	E_a / eV	N_T / cm^{-3}		σ_n / cm^2	Possible defect
P_1		22.2	0.02821	6.34×10^{12}		1.03×10^{-14}	Cs_i^{1+}
P_2		37.5	0.05428	1.53×10^{13}		1.61×10^{-14}	Pb_{Br}^{1+}
P_3	P_{3-1}	50.6	0.07851	1.48×10^{13}		1.17×10^{-14}	V_{Br}^{1+}
	P_{3-2}	59.3	0.09513	5.83×10^{13}	1.84×10^{14}	1.58×10^{-15}	
	P_{3-3}	71.3	0.11911	1.11×10^{14}		4.76×10^{-16}	
P_4	P_{4-1}	87.3	0.15178	1.07×10^{14}	1.20×10^{14}	1.59×10^{-16}	V_{Cs}^{1-}
	P_{4-2}	96.8	0.17183	1.28×10^{13}		2.35×10^{-15}	
P_5		117.1	0.21540	3.92×10^{13}		2.02×10^{-17}	Pb_i^{1+}
P_6		158.2	0.30762	7.70×10^{12}		1.33×10^{-16}	Pb_i^{2+}
P_7		232.1	0.48175	1.12×10^{13}		1.84×10^{-17}	Pb_{Br}^{2+}
Total				3.84×10^{14}			

Trap P_1, with an activation energy of 0.02821 eV, is identified as Cs_i^{+}. Trap P_2, with an activation energy of 0.05428 eV, is identified as Pb_{Br}^{1+} or Br_i^{1-}, but the possibility of Br_i^{1-} is relatively small in the melt-grown crystal because of the high Br vapor pressure [4] . Trap P_3 (for SIMPA best fitting P_{3-1}, P_{3-2} and P_{3-3} with similar activation energies of 0.0781eV, 0.09513eV and 0.11911eV, respectively) is identified as V_{Br}^{1+} or Br_{Cs}^{1-} defect. However, the Br_{Cs}^{1-} defect is hard to form (the lack of Br_i^{1-}). Trap P_4 (for SIMPA best fitting P_{4-1} and P_{4-2} with similar activation energies of 0.15178eV and 0.17183eV, respectively) is identified as V_{Cs}^{1-}. Trap P_5, with an activation energy of 0.21540 eV, is identified as Pb_i^{1+}. Trap P_6, with an activation energy of 0.30762 eV, is identified as Pb_i^{2+}. And Trap P_7, with an activation energy of 0.48175 eV, is identified as Pb_{Br}^{2+}.

Table S4. Defect-related parameters based on the best fit of a TSC spectrum of a sample from the middle part of a stoichiometric $CsPbBr_3$ ingot

Peak level (T)		T_m / K	E_a / eV	N_T / cm^{-3}		σ_n / cm^2	Possible defect
P_1		19.22	0.02341	1.34×10^{12}		8.41×10^{-15}	Cs_i^{1+}
P_2	$P_{2\text{-}1}$	32.95	0.04624	4.10×10^{11}	7.49×10^{11}	1.11×10^{-14}	Pb_{Br}^{1+}
	$P_{2\text{-}2}$	38.13	0.05543	3.39×10^{11}		2.93×10^{-14}	
P_3	$P_{3\text{-}1}$	76.48	0.12951	2.35×10^{13}	3.89×10^{13}	4.76×10^{-15}	V_{Cs}^{1-}
	$P_{3\text{-}2}$	80.83	0.13843	1.53×10^{13}		2.06×10^{-15}	
P_4		117.5	0.21635	1.35×10^{11}		6.88×10^{-16}	Pb_i^{1+}
P_5	$P_{5\text{-}1}$	250	0.52541	2.22×10^{14}	3.71×10^{14}	5.02×10^{-17}	Pb_{Br}^{2+}
	$P_{5\text{-}2}$	250	0.52541	5.89×10^{13}		3.13×10^{-16}	
	$P_{5\text{-}3}$	250	0.52541	9.01×10^{13}		6.18×10^{-18}	
Total				4.12×10^{14}			

Table S5. Defect-related parameters based on the best fit of a TSC spectrum of a sample from the tail part of a stoichiometric $CsPbBr_3$ ingot

Peak level (T)		T_m / K	E_a / eV	N_T / cm^{-3}		σ_n / cm^2	Possible defect
P_1		98.27	0.17491	1.34×10^{13}		2.17×10^{-16}	V_{Cs}^{1-}
P_2	$P_{2\text{-}1}$	144.8	0.27705	3.71×10^{14}	1.27×10^{15}	5.09×10^{-16}	Pb_i^{1+}
	$P_{2\text{-}2}$	153.5	0.29688	1.38×10^{14}		6.64×10^{-16}	
	$P_{2\text{-}3}$	153.5	0.29688	7.57×10^{14}		4.36×10^{-17}	
P_3		197.0	0.39792	6.68×10^{13}		2.28×10^{-16}	Pb_i^{2+}
P_4		225.6	0.46616	7.51×10^{13}		2.78×10^{-17}	Pb_{Br}^{2+}
P_5	$P_{5\text{-}1}$	262.9	0.55708	3.59×10^{14}	9.30×10^{14}	2.33×10^{-17}	Pb_{Br}^{3+}
	$P_{5\text{-}2}$	278.0	0.59431	3.04×10^{14}		5.54×10^{-17}	
	$P_{5\text{-}3}$	286.6	0.61587	1.87×10^{14}		1.30×10^{-16}	
	$P_{5\text{-}4}$	292.4	0.63042	7.99×10^{13}		3.04×10^{-16}	
Total				2.35×10^{15}			

Table S6. Defect-related parameters based on the best fit of a TSC spectrum of a sample from the tip part of a 1% Pb-poor $CsPbBr_3$ ingot

Peak level (T)		T_m / K	E_a / eV	N_T / cm^{-3}		σ_n / cm^2	Possible defect
P_1		22.47	0.02857	5.65×10^{13}		3.09×10^{-15}	Cs_i^{1+}
P_2	P_{2-1}	43.07	0.06441	2.66×10^{13}	4.41×10^{13}	1.63×10^{-15}	V_{Br}^{1+}
	P_{2-2}	55.83	0.08848	1.75×10^{13}		1.97×10^{-15}	
P_3		80.86	0.13848	9.45×10^{13}		2.45×10^{-16}	V_{Pb}^{2-} or Cs_{Pb}^{1-}
P_4		118.7	0.21901	7.71×10^{13}		1.84×10^{-16}	Pb_i^{1+}
P_5	P_{5-1}	137.0	0.25961	6.11×10^{13}	3.80×10^{14}	5.02×10^{-16}	Pb_i^{2+}
	P_{5-2}	150.2	0.28920	1.24×10^{14}		3.97×10^{-16}	
	P_{5-3}	162.2	0.31669	1.82×10^{14}		5.80×10^{-16}	
	P_{5-4}	175.7	0.34781	1.20×10^{13}		3.07×10^{-16}	
P_6		196.3	0.39620	2.08×10^{13}		4.56×10^{-17}	Pb_{Br}^{2+}
P_7	P_{7-1}	241.3	0.50422	6.91×10^{13}	1.45×10^{14}	3.64×10^{-17}	Pb_{Br}^{3+}
	P_{7-2}	247.3	0.51880	7.63×10^{13}		7.01×10^{-18}	
Total				8.18×10^{14}			

Table S7. Defect-related parameters based on the best fit of a TSC spectrum of a sample from the tip part of a 1% Pb-rich $CsPbBr_3$ ingot

Peak level (T)		T_m / K	E_a / eV	N_T / cm^{-3}		σ_n / cm^2	Possible defect
P_1		22.90	0.02926	3.97×10^{16}		5.31×10^{-15}	Cs_i^{1+}
P_2		38.26	0.05565	7.76×10^{16}		4.93×10^{-16}	Pb_{Br}^{1+}
P_3	P_{3-1}	96.86	0.17192	1.57×10^{17}	1.69×10^{17}	2.28×10^{-17}	V_{Cs}^{1-}
	P_{3-2}	96.86	0.17192	1.19×10^{16}		3.57×10^{-16}	
P_4	P_{4-1}	251.7	0.52960	6.19×10^{17}	1.29×10^{18}	2.19×10^{-17}	Pb_{Br}^{2+}
	P_{4-2}	251.7	0.52960	6.70×10^{17}		6.49×10^{-17}	
Total				1.57×10^{18}			

REFERENCES

(1) Zhang, M.; Zheng, Z.; Fu, Q.; Chen, Z.; He, J.; Zhang, S.; Yan, L.; Hu, Y.; Luo, W. Growth and characterization of the all-inorganic lead halide perovskite semiconductor $CsPbBr_3$ single crystals. *CrystEngComm*. **2017**, 19(45), 6797-6803.

(2) Kang, J.; Wang, L. W. High Defect Tolerance in Lead Halide Perovskite $CsPbBr_3$. *J. phys. Chem. Lett*. **2017**, 8(2), 489-493.

(3) Look, D. C. Chapter 2 The Electrical and Photoelectronic Properties of Semi-Insulating GaAs, *Semiconduct. Semimet*. **1983**, 19, 75-170.

(4) Mansour, A. E.; Dey, S.; Amassian, A.; Tanielian, M. H. Bromination of graphene: a new route to making high performance transparent conducting electrodes with low optical losses. *ACS Appl. Mater. Inter.* **2015**, 7(32), 17692-17699.